Electrocatalytic properties of the catalysts based on carbon nanofibers with various platinum contents

E. V. Gerasimova, N. G. Bukun, and Yu. A. Dobrovolsky*

Institute of Problems of Chemical Physics, Russian Academy of Sciences, 1 prosp. Akad. Semenova, 142432 Chernogolovka, Moscow Region, Russian Federation. Fax: +7 (496) 522 5401. E-mail: lyramail@mail.ru

The catalysts on carbon nanofibers with various platinum contents were synthesized. The morphology, resistance to oxidation, and electrochemical behavior of the catalysts in the reactions that occur in fuel cells were studied. The dependence of the specific output of cathodes of hydrogen—air fuel cells on the sizes of the platinum clusters was established.

Key words: carbon nanofibers, Pt/C catalysts, fuel cells, size effect.

The problem of development and investigation of the catalyst for oxygen reduction became topical in the recent time from both theoretical and practical points of view. The absence of cheap corrosionproof cathodic catalysts is a major barrier for commercialization of low-temperature fuel cells (FC). For the development of theoretical concepts, it is important to study reasons for the appearance of the size effect, to determine the particle size optimum for catalysis, and to study the nature of their interaction with the support.

Catalysts based on platinum and its alloys are nearly the only active catalytic systems for oxygen electroreduction at low temperatures in acidic media. In the first years of development of the technology of low-temperature FC, Pt black was used as a cathode for the catalyst (with the loading about 30 mg cm^{-2} and the typical Pt particle size range 5—30 nm). Currently, platinum supported on carbon black is used, which made it possible to decrease the catalyst loading about two orders of magnitude.

It became possible to develop catalysts based on carbon black due to the stabilization of platinum on the support surface as nanosized clusters (2—10 nm), whose specific catalytic activity depends on the particle size ("size effect").[1] There were several attempts to explain a similar phenomenon by specific features of the electronic structure of the catalyst, the number of atoms with the low coordination number, the predominant crystallographic orientation, and the existence of defects. Probably, the simultaneous influence of factors of this kind on the activity of the catalyst is a reason for ambiguous results of the search for the optimum relation between the catalyst morphology and catalytic activity. It was shown[2,3] for the oxidation of hydrogen that the optimum size of the Pt crystallite is 2—3 nm and that for the reduction of oxygen is 2—4 nm.[4,5] However, it is shown in some works that no size effect is observed for the platinum crystallites larger than 1.4 nm.[6—8] Chronoamperometric procedures were proposed in several works for the study of the activity of platinum nanoclusters. It was shown that the areas of intergrain boundaries contribute considerably to the activity.[9]

Nanostructured carbon materials (nanotubes (CNT), nanofibers (CNF)) and diverse oxide supports are used along with carbon black as catalyst supports. The low cost, high conductivity, good mechanical properties, and the resistance to oxidation, which is higher than that of carbon black, are usually referred to advantages of carbon nanofibers. The extended structure of the CNF favors the improvement of the properties of the catalytic layer in the fuel cell.

The surface functional groups of the carbon supports affect the formation, dispersity, and strength of the bond with the support of reduced small platinum particles (2—4 nm). In addition to the catalytic activity, an important characteristic of the active FC layer is its stability in time. The decomposition of the active layer can be related to the agglomeration of particular platinum clusters. Therefore, the authors of several works[10—16] believe that the chemical modification of the carbon surface by, for example, carboxyl and thiol groups makes it possible to anchor the metal on the support surface. However, the oxidation of CNF results in the formation of unbound residual modifying molecules, which complicate a further interpretation of the electrochemical behavior of the prepared catalysts and which may exert a negative effect on the electroconducting properties of the support.[17—19]

The purpose of this work is to study the influence of the composition of Pt/CNF and the platinum cluster size on the electrochemical properties of the catalyst.

Published in Russian in *Izvestiya Akademii Nauk. Seriya Khimicheskaya,* No. 6, pp. 1021—1026, June, 2011.

1066-5285/11/6006-1045

Experimental

Carbon nanofibers with a diameter of 100—200 nm, a length of 1—5 μm, and a specific surface of the 100 $m^2 g^{-1}$ BET (N_2) were used as platinum supports.[20] According to the elemental analysis data, the oxygen content is lower than 0.5%.

Platinum was supported on carbon fibers by the reduction of $PtCl_6^{2-}$ in an alkaline solution of ethylene glycol (pH 11) under the action of microwave radiation (800 W, 1 min). The synthesized samples of the Pt/C catalysts were filtered and dried for 10 h at 105 °C in a desiccator. Thermogravimetric (TGA) and differential thermal (DTA) analyses were carried out using an STA 409 Luxx thermoanalyzer with the mass spectrometric attachment for analysis of gaseous products (Netzsch). The TGA and DTA curves were recorded in the linear heating regime at 10 °C min^{-1} from room temperature to 1000 °C in an air flow (flow rate 50 mL min^{-1}). Weighed samples (5—10 mg) were placed in a corundum crucible, and the platinum content was determined by the incombustible residue at the end of experiment. The samples with the weight content of platinum from 4% to 61% were obtained by the variation of the Pt : C ratio.

The specific surface of materials was determined by the BET method on a Quadrasorb SI instrument (Quantachrome). The pore size distribution was constructed on the basis of the analysis of the curves of nitrogen sorption/desorption.[21,22]

The platinum particle sizes were determined by transmission electron microscopy (TEM) (Zeiss LEO 912B) and using powder X-ray diffraction (Brucker D8 Advances, $K\alpha_1$ monochromator, 1D detector, $CuK\alpha_1$ radiation). An analysis of the microimages of the catalysts made it possible to construct the average-numerical particle-size distributions for platinum (200—500 units), accepting that the particles were spherical and ignoring agglomerates. To obtain the average-mass distribution, the weight was calculated for each measured particle.

For electrochemical studies of the catalysts, the electrodes were prepared as follows. Carbon nanofibers with supported platinum were dispersed in water with the addition of dispersion Nafion® DE1020 (DuPont, USA) in an amount of 25% of the carbon weight and were supported in the surface of the gas-diffusion layer Toray® TGP-H-060 (Toray Industries, Inc., Japan). The prepared electrode was used as a working electrode in the three-electrode cell, and a reversible hydrogen electrode (0.5 *M* H_2SO_4, 20 °C) served as a reference. Prior to measurements of carbon monoxide adsorption, background voltammograms were detected on the electrode under study in the potential range from 0.1 to 1.2 V with a potential sweep of 0.02 V s^{-1}. The true surface of the electrodes was calculated by the surface area of the desorption peak of carbon monoxide. For this purpose, the solution in the cell was saturated with CO for 15 min at an electrode potential of 0.1 V, then CO was removed by blowing with argon, and cyclic voltammograms were detected. All potentials are presented relatively to the reversible hydrogen electrode taking into account ohmic losses, which were determined by the impulse potentiostatic method (inaccuracy 3%).

The electrodes of fuel cells were studied in the reduction of oxygen in a liquid gas-diffusion half-cell (1 *M* H_2SO_4) by cyclic and stationary voltammetry (as stationary were taken the values of current detected 30 min after the moment at which specified potential was attained). The reversible hydrogen electrode was used as a reference electrode, and a glassy carbon plate served as a reference electrode. The measurements were carried out according to the procedure described earlier.[23]

Results and Discussion

The synthesized samples Pt/CNF with a weight content of platinum of 4—61% were studied by transmission electron microscopy. The microimages of the samples with the platinum content 4, 12, and 49% are shown in Fig. 1. The platinum particles are uniformly distributed over the surface of carbon fibers. It is seen that the number of large clusters increases with an increase in the platinum content. The Pt cluster size distribution (Fig. 2) calculated by the TEM data is described by the log-normal distribution typical of freely growing particles.[24,25] The average-mass distribution is broader than the average-numerical one, and this difference increases with an increase in the platinum content. Assuming that the nanoparticles are spherical, the specific surface S_{geom} was calculated for all catalysts (Table 1).

The prepared catalysts were also characterized by powder X-ray diffraction (Fig. 3). The platinum content in the studied samples exerts a noticeable effect on the diffraction patterns. All reflections of platinum in the region studied are well seen in the samples with a high platinum content. For the samples with a low platinum content, the reflection intensity from the carbon nanofibers is much higher than that from the platinum nanoparticles, and only one peak of platinum corresponding to the reflection [111] is observed. Based on the X-ray diffraction patterns ob-

Table 1. Characteristics of the Pt/CNF catalysts with various platinum contents

Content of Pt/(wt.%)	j^a/A (mg of Pt)$^{-1}$ (0.5 V)	S_{CO}	S_{geom}	D_N	D_M	D_{XRD}[b]
		$m^2 g^{-1}$			nm	
4	0.32	30	250	1.0	1.2	—[c]
7	3.05	90	120	2.1	2.6	2.5(40°)
12	2.61	120	125	2.0	2.5	—[c]
23	0.75	90	155	1.7	2.1	2.3(40°)
34	1.08	25	50	4.1	6.3	6.3(67°)
49	0.31	30	85	2.4	3.8	3.4(67°)
61	0.60	40	70	2.6	4.3	3.7(67°)

[a] At a potential of 0.5 V.

[b] Calculation by the Sherrer equation, $D = 0.9 \cdot 0.5406/V \cos\theta$, the value of 2θ is given in parentheses.

[c] The reflections corresponding to Pt are comparable with the background.

Note. D_N and D_M are the average-numerical and average-mass sizes of the platinum clusters; and D_{XRD} is the size of the Pt clusters determined by X-ray diffraction analysis.

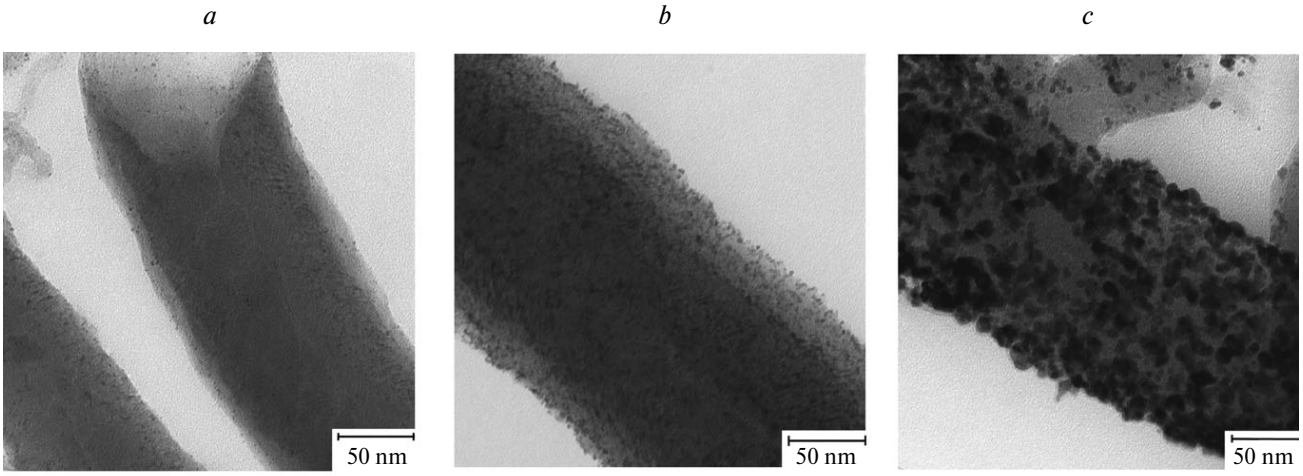

Fig. 1. Microimages of the Pt/CNF samples with the platinum content 4 (*a*), 12 (*b*), and 49 wt.% (*c*).

tained, the size of platinum crystallites was determined assuming that the particles are cubic with the very narrow size distribution.

The average-mass distributions better correspond to the X-ray phase analysis results.

The thermal resistance of the prepared catalysts to oxidation was studied by thermogravimetry. The temperature of the onset of sample oxidation was chosen as a parameter that characterizes resistance. It was shown that the resistance of the prepared samples decreases monotonically with an increase in the platinum content and is close to the resistance of the catalysts based on carbon black Vulcan XC-72 for the samples with the same platinum content (Fig. 4).

The combustion of carbon unbound with Pt occurs in the temperature range from 530 to 600 °C. As can be seen from Fig. 4, no considerable decrease in the temperature of the onset of carbon oxidation is observed when an increase in the platinum content exceeds 20%, apparently metal particles cover the carbon surface in an optimal way, regardless of the nature of the support (CNF, carbon black).

In order to simulate cathodic and anodic processes in the FC, the materials obtained were studied in a liquid

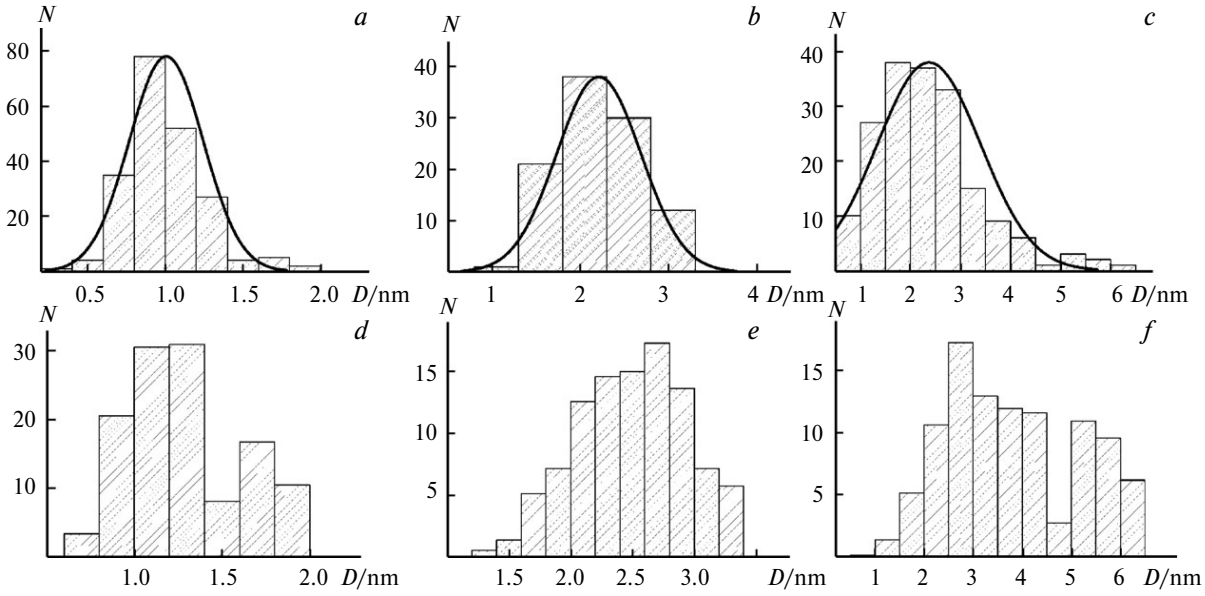

Fig. 2. Numerical (*a*—*c*) and weight (*d*—*f*) distributions of platinum clusters in the Pt/CNF samples with the platinum content 4 (*a*, *d*), 12 (*b*, *e*), and 49 wt.% (*c*, *f*) calculated by the TEM data. *N* is the number of clusters, and *D* is the cluster size.

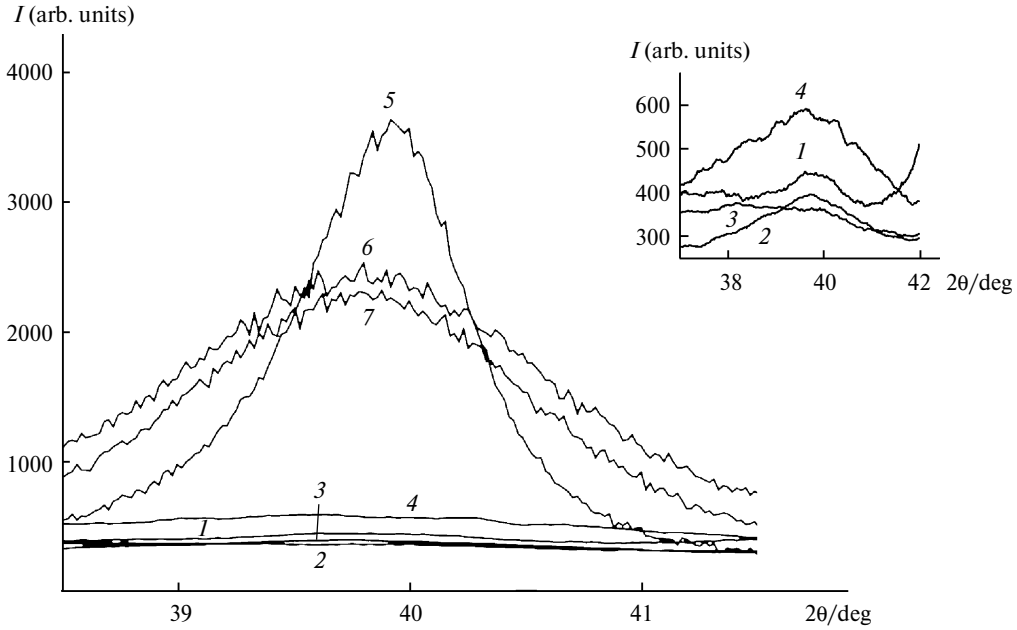

Fig. 3. XRD peak corresponding to the reflection from the plane [111] of the Pt crystallites of the synthesized catalysts Pt/CNF containing 4 (*1*), 7 (*2*), 12 (*3*), 23 (*4*), 34 (*5*), 49 (*6*), and 61 wt.% (*7*) of platinum. Curves (*1*)—(*4*) in the magnified scale are shown in inset.

gas-diffusion half-cell, which makes it possible to study the processes of oxygen reduction and hydrogen oxidation that occur independently in a fuel cell.[23] The multistep reaction of oxygen reduction is rate-determining in a hydrogen—air fuel cell. Therefore, to reveal the influence of the morphology of catalytic particles on the rate of the cathodic process, we recorded the stationary voltammetric curves of oxygen reduction on the prepared catalysts. The current densities on the catalysts in the reaction of oxygen reduction at a potential of 0.5 V were calculated to compare the working efficiency of the catalysts studied (see Table 1). It is shown that the dependence of the characteristics of the oxygen process on the platinum content in the catalyst can be described by a curve with the maximum, and the optimum Pt content is about 8—12%. However, the extreme mode of the obtained dependences is the manifestation of the size effect (Fig. 5), which depends on both the nature of surface defects and kinetic regularities of the reaction on the catalyst surface.

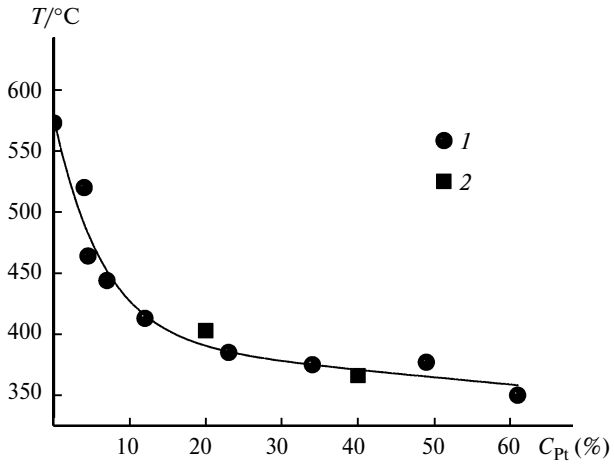

Fig. 4. The temperature of the onset of combustion of the catalysts based on the carbon nanofibers Pt/CNF (*1*) and carbon black Pt/XC-72 (*2*) *vs* platinum content (C_{Pt}) in the material.

The true surface of platinum was also determined by the materials Pt/CNF from the surface area of the CO desorption peak (see Table 1). A comparison of the values of S_{CO} with S_{geom} calculated from the size distributions of the surfaces showed that the results of the both methods for surface determination are poorly consistent when they are used for the estimation of platinum particles with the diameter lower than 2 nm. The same observation was made by the authors of Ref. 4. It is known that the specific catalyst surface increases sharply with a decrease in the particle size, which becomes especially pronounced for the crystallites with the sizes smaller than 2 nm. Thus, it could be expected that the electrochemical activity, which is directly affected by the number of surface atoms, should increase sharply with a decrease in the particle size. However, this does not correspond to the data presented in Fig. 5. It is possible that a part of the cluster surface is inactive, because the particles are incorporated in the pores of the carbon support and/or the

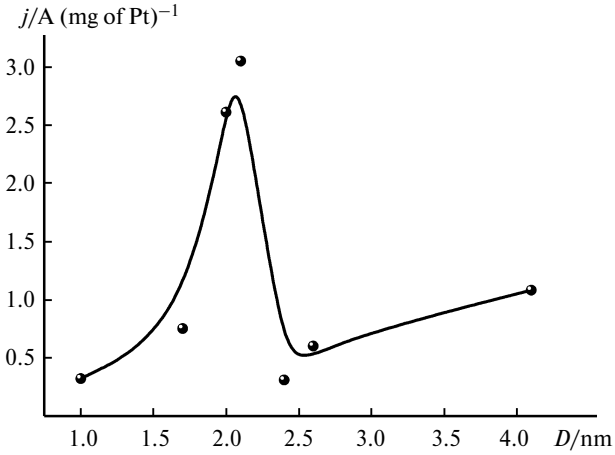

Fig. 5. Current density (*j*) *vs* size of the metal clusters (*D*) for the catalysts Pt/CNF at a potential of 0.5 V.

surface platinum atoms are deactivated by the surface groups of the support.

To check this assumption, we measured nitrogen adsorption and desorption on the initial CNF and on the CNF-based catalyst. The plots of the pore volume *vs* diameter are presented in Fig. 6. The results of the analysis show that the most part of pores in the initial nanofibers have the size from 1 to 2 nm, whereas these pores disappear in the fibers with supported platinum. This suggests that nucleation starts in pores of the carbon support and continues until the cluster size would be comparable with the pore size. As a result, the particle that formed becomes incapable of efficient catalyzing electrochemical processes.

In the present work, the samples of Pt/CNF with various platinum content were prepared by the polyol method. Their morphology, thermal stability, and electroactivity in the reaction of oxygen reduction were studied. It was found that the resistance of the materials to oxidation

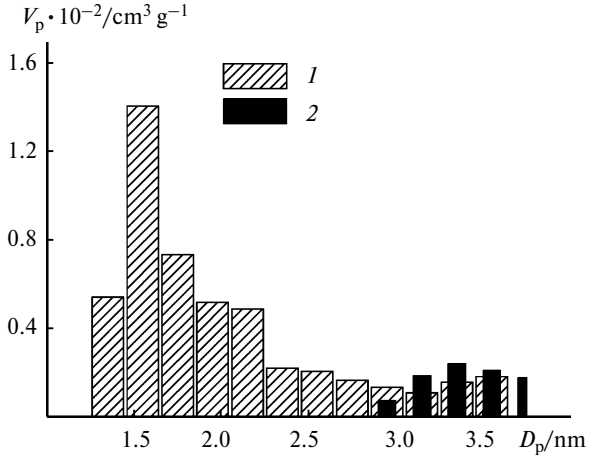

Fig. 6. Micropore size distribution for the initial CNF (*1*) and catalyst Pt/CNF with the platinum content 4 wt.% (*2*).

decreases monotonically with an increase in the amount of platinum. The dependence of the specific power of the cathode based on the prepared catalysts on the platinum cluster size can be described by the curve with the maximum. The presence of micropores on the support surface was shown to exert a substantial effect on the electrochemical behavior of small platinum clusters ($d \leq 2$ nm). The effect indicates that some metal particles with the size smaller or comparable with the pore size of the carbon fiber are blocked by fibers. The results obtained in the work suggest that the Pt/C electrocatalysts with the platinum content 7—12 wt.% and the particle size 2—3 nm are most promising among the catalysts based on carbon nanofibers.

The carbon nanofibers were kindly presented by A. A. Volodin (Institute of Problems of Chemical Physics, Russian Academy of Sciences). The authors are grateful to I. S. Bushmarinov (N. A. Nesmeyanov Institute of Organoelement Compounds, Russian Academy of Sciences) for X-ray diffraction studies.

This work was financially supported by the Russian Foundation for Basic Research (Project No. 09-03-01157a).

References

1. *Catalysis and Electrocatalysis at Nanoparticle Surfaces*, Eds A. Wieckowski, E. R. Savinova, C. G. Vayenas, Marcel Dekker, New York, 2003, 970 pp.
2. J. Lipkowski, P. N. Ross, *Electrocatalysis*, Wiley-VCH, New York, 1998, p. 197.
3. P. H. Lewis, *J. Phys. Chem.*, 1963, **67**, 2151.
4. K. Makino, M. Chiba, T. Koido, *Meet. Abstr. — Electrochem. Soc.*, 2010, **1002**, 647.
5. L. Gan, H. Du, B. Li, F. Kang, *New Carbon Mater.*, 2010, **25**, 53.
6. M. Watanabe, H. Sei, P. Stonehart, *J. Electroanal. Chem.*, 1989, **261**, 375.
7. M. Watanabe, S. Saegusa, P. Stonehart, *Chem. Lett.*, 1988, **17**, 1487.
8. M. Watanabe, S. Saegusa, P. Stonehart, *J. Electroanal. Chem.*, 1989, **271**, 213.
9. O. V. Cherstiouk, A. N. Gavrilov, L. M. Plyasova, I. Yu. Molina, G. A. Tsirlina, E. R. Savinova, *J. Solid State Electrochem.*, 2008, **12**, 497.
10. Zh. Liu, X. Lin, J. Y. Lee, W. Zhang, M. Han, L. M. Gan, *Langmuir*, 2002, **18**, 4054.
11. H. Hiura, T. W. Ebbesen, K. Tanigaki, *Adv. Mater.*, 1995, **7**, 275.
12. D. S. Bag, R. Dubey, N. Zhang, J. Xie, V. K. Varadan, D. Lal, G. N. Mathur, *Smart Mater. Struct.*, 2004, **13**, 1263.
13. X. Li, I.-M. Hsing, *Electrochim. Acta*, 2006, **51**, 5250.
14. Y.-T. Kim, K. Ohshima, K. Higashimine, T. Uruga, M. Takata, H. Suematsu, T. Mitani, *Angew Chem., Int. Ed.*, 2006, **45**, 407.
15. J. K. Lim, W. S. Yun, M. Yoon, S. K. Lee, C. H. Kim, K. Kim, S. K. Kim, *Synth. Met.*, 2003, **139**, 521.

16. X. Sun, R. Li, D. Villers, J. P. Dodelet, S. Désilets, *Chem. Phys. Lett.*, 2003, **379**, 99.
17. D. Sebastián, I. Suelves, R. Moliner, M. J. Lázaro, *Carbon*, 2010, **48**, 4421.
18. D. Pantea, H. Darmstadt, S. Kaliaguine, L. Sümchen, C. Roy, *Carbon*, 2001, **39**, 1147.
19. D. Pantea, H. Darmstadt, S. Kaliaguine, C. Roy, *Appl. Surf. Sci.*, 2003, **217**, 181.
20. A. A. Volodin, P. V. Fursikov, Yu. A. Kasumov, I. I. Khodos, B. P. Tarasov, *Izv. Akad. Nauk, Ser. Khim.*, 2005, 2210 [*Russ. Chem. Bull., Int. Ed.*, 2005, **54**, 2281].
21. P. Tarazona, U. Marini Bettolo Marconi, R. Evans, *Mol. Phys.*, 1987, **60**, 573.
22. J. Jagiello, D. Tolles, in *Fundamentals of Adsorption*, Ed. F. Meunier, Elsevier, Paris, 1998, vol. **6**, p. 629.
23. E. A. Astaf´ev, Yu. A. Dobrovolsky, E. V. Gerasimova, A. V. Arsatov, *Al´ternativnaya energetika i ekologiya* [*Alternative Power Engineering and Ecology*], 2008, No. 2, 86 (in Russian).
24. L. B. Kiss, J. Söderlund, G. A. Niklasson, C. G. Granqvist, *Nanotechnology*, 1999, **10**, 25.
25. C. G. Granqvist, R. A. Buhman, *J. Appl. Phys.*, 1976, **47**, 2200.

Received March 4, 2011;
in revised form June 6, 2011